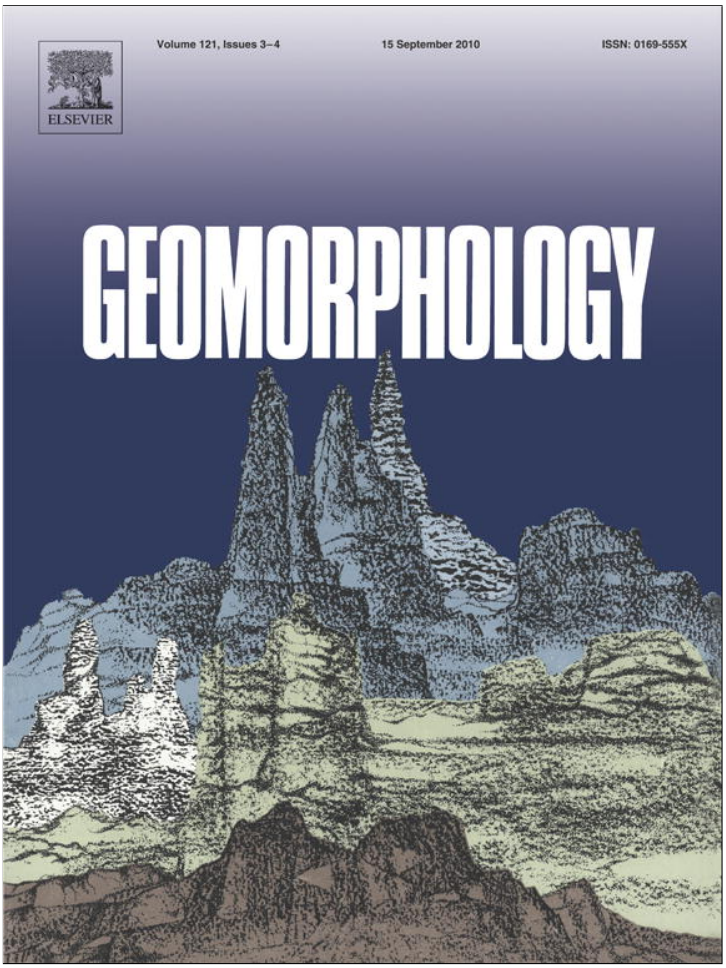

Geomorphology 121 (2010) 257–265

Contents lists available at ScienceDirect

Geomorphology

journal homepage: www.elsevier.com/locate/geomorph

# Sand transport on an estuarine submarine dune field

Eduardo A. Gómez [a,b], Diana G. Cuadrado [a,c,*], Jorge O. Pierini [a,d]

[a] CONICET-Instituto Argentino de Oceanografía (IADO), CC804, 8000 Bahía Blanca, Argentina
[b] UTN Regional Bahía Blanca, 11 de Abril 360, 8000 Bahía Blanca, Argentina
[c] Dto. Geología, Universidad Nacional del Sur (UNS), San Juan 670, 8000 Bahía Blanca, Argentina
[d] Dto. de Física, Universidad Nacional del Sur (UNS), Avda Alem 1253, 8000 Bahía Blanca, Argentina

ARTICLE INFO

*Article history:*
Received 20 October 2009
Received in revised form 6 April 2010
Accepted 27 April 2010
Available online 12 May 2010

*Keywords:*
Sand dunes
ADCP profiles
Dune migration
Swath bathymetry system

ABSTRACT

By means of surveys carried out with a Phase Measuring Bathymetric System and current profiles obtained through an ADCP of the internal area of the Bahía Blanca estuary, a field of large dunes was analysed. There are two different and well-defined zones characterized by particular dune morphology and differing hydrodynamics. The reduction in the channel cross-section by a geological control leads to the increase in tidal current velocity, which together with the available sediment leads to the formation of Very Large Dunes ($H$>4 m and $L$>100 m) with the typical morphology of a limited amount of sediment overlying a rigid substrate. The migration rate of these dunes, between 65 and 130 m year$^{-1}$, decreases as the bedform height increases. Differing sediment transport rates across the channel result in a non-uniform migration rate, which is responsible for the formation of dunes with linear crests oblique to the tidal current direction. This fact indicates that determination of the sediment transport direction by using only large bedform orientation may be subject to a significant error.



## 1. Introduction

The bottom morphology of an estuary is directly related to the sediment and fluid dynamics and thus yields complementary information for the evaluation of the sediment budget and transport. This is one of the reasons why flow-transverse bedforms have remained the subject of extensive research (Flemming, 1978; Ashley, 1990; Harbor, 1998; Carling et al., 2000).

Dunes are a major sediment transport mechanism in many subaerial (eolian) and subaqueous (marine or fluvial) environments (Allen, 1982). In the latter case, they develop as a result of an inherent instability of sand beds forced by water flows (Besio et al., 2004); thus, the size, shape, and other properties of the dunes depend on the driving force, water depth, and sediment grain size (Rubin and McCulloch, 1980; Ashley, 1990; Francken et al., 2004; Bartholdy et al., 2005). Large dunes are, generally, the result of abundant sediment availability and strong currents capable of inducing bedload movement (Bastos et al., 2004).

Only recently have surveys with advanced sounding and navigational technology revealed the detailed morphology of large dunes in 3D (Xu et al., 2008). Such high-resolution swath bathymetry at centimeter-scale accuracy enables researchers to study the spatial variation in a very precise manner and to examine temporal changes. Furthermore, the bathymetric data provides researchers with the opportunity to characterize the lateral (across-channel) variations of dunes (Ernstsen et al., 2005). Nowadays, multibeam sonar systems are commonly used. They not only provide sea-floor bathymetry and morphology, but also acoustic backscatter data that can reveal significant information for indirect sea-floor characterization (Mitchell, 1996; Goff et al., 2004). For the present study, a Phase Measuring Bathymetric System (PMBS) "GeoSwath Plus" from GeoAcoustics Ltd., UK was used. This system works in a similar manner as multibeam sonar, but with only a pair of transducers and measuring the phase difference of the backscattered acoustic signals in order to compute distances and angles to determine lateral depths.

To understand the dynamics of subaqueous dunes, numerous studies have been carried out in rivers (Sukhodolov et al., 1998; Carling et al., 2000), in tidal environments (Dalrymple et al., 1978; Kostaschuk, et al., 1989; Harbor, 1998) and on the continental shelf (Flemming, 1978; Ardhuin et al., 2002). All these environments inferred high energy forces. Some years ago, a dune field was studied in the mesotidal Estuary of Bahia Blanca (Cuadrado et al., 2003; 2005) characterized by the presence of Very Large Dunes, following the classification of Ashley (1990). This type of dunes is of an unusual scale to be found in this kind of environment.

A high-precision bathymetric map and the measured hydrodynamic regime allow us to distinguish between the various hypotheses previously considered for the formation of Very Large Dunes. The objective of this paper, therefore, is to analyse the dynamics of the

* Corresponding author. CONICET-Instituto Argentino de Oceanografía (IADO), CC804, 8000 Bahía Blanca, Argentina. Tel.: +54 291 4861666 int 162; fax: +54 291 4861519.
*E-mail addresses:* gmgomez@criba.edu.ar (E.A. Gómez), cuadrado@criba.edu.ar (D.G. Cuadrado), jpierini@criba.edu.ar (J.O. Pierini).

0169-555X/$ – see front matter © 2010 Elsevier B.V. All rights reserved.
doi:10.1016/j.geomorph.2010.04.022

area in order to determine why Very Large Dunes are present in a mesotidal estuary. Thus, the paper documents the spatial and temporal distribution of these bedforms and tries to understand their formation mechanism.

## 2. Study area

The Bahía Blanca estuary is located in the south of Buenos Aires province, Argentina. It has a mesotidal semi-diurnal regime, with a mean tidal range from 2.5 m at the mouth to more than 4 m at its head. On the north coast of the estuary is the most important deep-harbour complex of Argentina, connected to the open ocean through a 100 km-long access channel (Fig. 1). However, several sections of this channel need to be frequently dredged in order to maintain navigational depths.

The estuary has a general triangular shape with a width of 53 km at the mouth, and can be described as series of major NW–SE tidal channels that separate extended tidal flats, marshes and islands. Perillo and Piccolo (1991) concluded that the Bahía Blanca estuary behaves hypersynchronously as tidal range and tidal current amplitude increase headward. Tidal currents are reversible with maximum velocities measured at the surface of about 1.3 m $s^{-1}$ and maximum vertically averaged values of 1.2 and 1.05 m $s^{-1}$ for ebb and flood conditions, respectively.

There are only two small fresh-water sources. Sauce Chico River (drainage area of 1600 $km^2$) outflows in the inner area and the Napostá Grande Stream in the middle zone of the estuary, with annual mean discharges of 1.9 and 0.8 $m^3$ $s^{-1}$, respectively (Cuadrado et al., 2005). Thus, the sediment input by fresh-water streams is negligible when compared to the amount of sediments circulating within the estuary. The main sediment source is the reworking of unconsolidated Quaternary deposits from the bed and banks of tidal channels, caused mainly by the strong tidal currents occurring in the environment and, to a lesser extent, by waves. In some parts, the sub-bottom of the estuary is characterized by consolidated and lithified rocks composed by reddish brown sandstone (Chasicó Fm.) of Pliocene age (Tertiary) that crops out with irregularities of up to 1.5 m in height (Perillo et al., 2009).

In the middle section of the Main Channel of the estuary, an important submarine dune field is recognized. This kind of bedform usually occurs in highly dynamic environments such as tidal inlets and macrotidal estuaries, not under a mesotidal regime as in the Bahía Blanca estuary.

## 3. Methods

Detailed bathymetry was performed by means of a PMBS, which yielded details and disposition of the bedforms present on the channel bed with 10° cm precision. This modern instrument offers wide swath coverage around 8 times the water depth to a maximum width of 600 m. Crosswise-track resolution is 1.5 cm, while lengthwise-track resolution depends on the rate of the swath and the vessel speed. It has one pair of 250 kHz transducers (suitable for up to 100 m water depth), a Meridian Gyro Compass to provide heading data, and a TSS DMS2-05 Motion Reference Unit (MRU) for measuring heave, pitch and roll.

Bathymetric lines were made along a general direction parallel to the channel axis (SE–NW) with a lateral overlap of the order of 50%. Sound velocity profiles through the water column were measured periodically during the surveys and applied to the data to prevent refraction errors. The depth data were inspected and erroneous values removed using the system's specific software (GS+ v 3.10). A total area of about 3 $km^2$ was surveyed, covering the entire channel up to a minimum depth of 4.5 m at the flanks. All bathymetric data were referred to the local datum plane by means of the tidal information from Puerto Belgrano tidal gauge. The bathymetric information was processed to obtain a 1-m grid spacing or bathymetric map, where profiles and all the parameters to characterize dunes (height, *H*; spacing, *S*; depth, d) were measured with sub-metre accuracy (see Fig. 2).

In order to determine dune migration rates, PMBS surveys were repeated eight months later where the Very Large Dunes occur, the crest position in both maps was compared and the distance of migration was measured.

Bottom sediment samples were obtained by means of a van Veen dredge. They were processed in the laboratory using a Malvern Multisizer 2000 Laser Particle Analyzer and the statistical parameters computed by means of the program GradiStat (Blott and Pye, 2001). Grain size analyses showed that all samples were composed of medium to coarse sand.

Tidal currents were measured using a BroadBand™ (RDI) acoustic Doppler current profiler (ADCP) mounted on a ship, operating at 600 kHz. The vertical resolution of the ADCP was set to 0.25 m. Lateral resolution was 5–10 m using a ping rate of 2 Hz and a vessel speed of 2.6 m $s^{-1}$ (5 kn). Currents were measured during a tidal cycle, obtaining the distribution of velocity through the water column over two tracks carried out transversally to the channel. Values were computed with the WinRiver™ (RDI) software package.

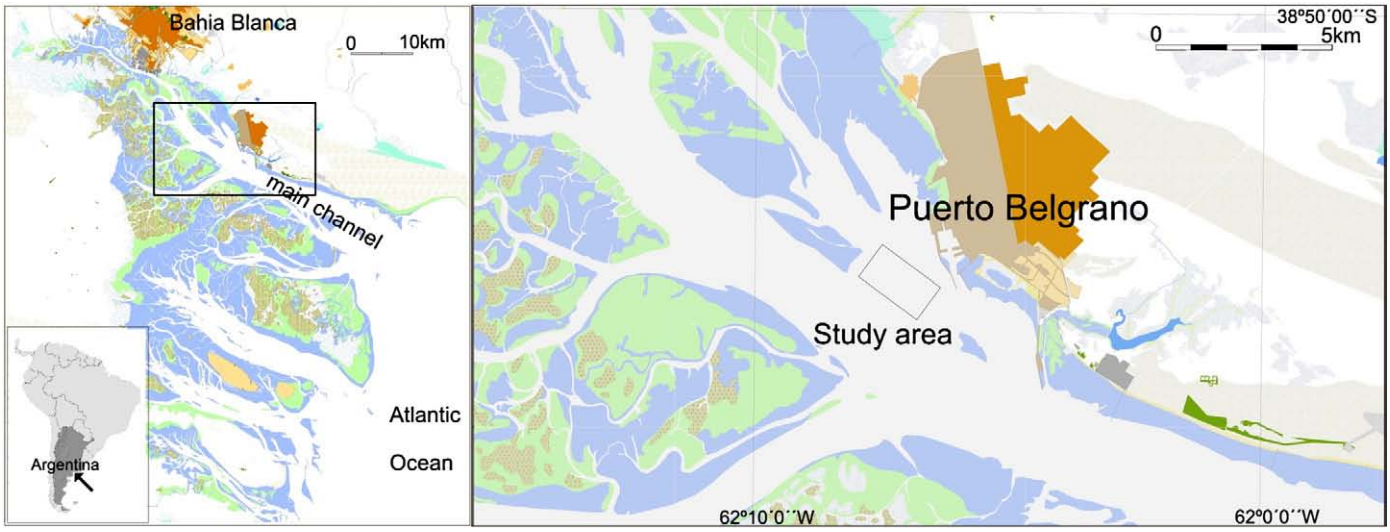


**Fig. 1.** Location of the study area in the Bahia Blanca estuary.

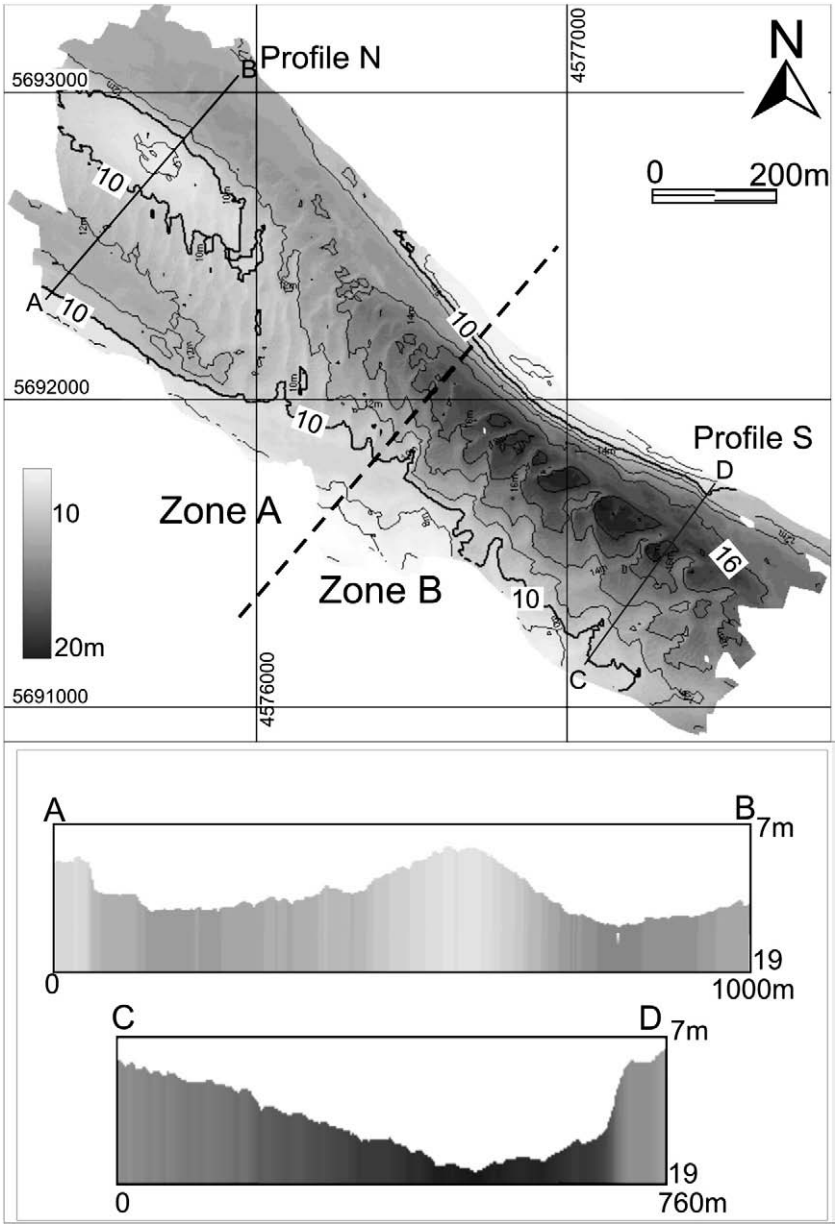


**Fig. 2.** Bathymetric map showing profiles N and S to characterize Zones A and B. The equidistance is 2 m. Coordinates are in Gauss Krüger projection (similar to UTM).

The entire fieldwork (PMBS, sampling and ADCP) was performed with the 14-m long boat "Buen Día Señor" that belongs to the Instituto Argentino de Oceanografia (IADO) positioned by means of a DGPS Sokkia Radian IS operating in RTK mode, which leads to bedform positioning errors of just a few centimetres.

## 4. Results and discussion

### *4.1. Dune field morphology*

The bathymetry of the surveyed area is shown in Fig. 2. The area exhibits a narrowing of the channel delimited by the 10 m isobath with mean depths of 10 m at the northwestern extreme and maximum depths greater than 18 m to the southeast, close to the northern flank. Two zones with different characteristics were distinguished in the area. Zone A, northwestern extreme of the surveyed area, exhibits a sand bank in the middle of the channel with shallower depths of 6 m (profile N). In the channels located on both sides of the bank, a maximum depth of 13–14 m occurs. Zone B, on the southeastern extreme, exhibits maximum depths greater than 18 m (profile S). Around the 10-m isobath, both channel flanks show hard to erode sediment strata which exhibit sharp steepness. Probably, these sediments would match to Chasicó Fm., which also outcrops in a nearby sector (Perillo, et al., 2009) at similar depths. These features can be clearly identified on profiles C–D and E–F of the bathymetric map presented in Fig. 3.

Otherwise, most of the surveyed area is covered with non-cohesive medium to coarse sand with very low percentages of fines, as is evidenced by the numerous observed bedforms. The two zones exhibit differing dune types. Medium and Large Dunes, according to the Ashley (1990) classification, were characteristic in Zone A (profiles G–H, Fig. 3). It is important to note that the linear crest of the larger dunes occurring in the middle part in Zone A exhibits a N–S orientation, which is an oblique disposition to the channel axis (white arrows in Fig. 3). The features develop into Very Large Dunes in Zone B, which are present only over the northern flank (see profiles A–B, Fig. 3), with heights ($H$) greater than 4 m and wavelengths ($L$) larger than 100 m.

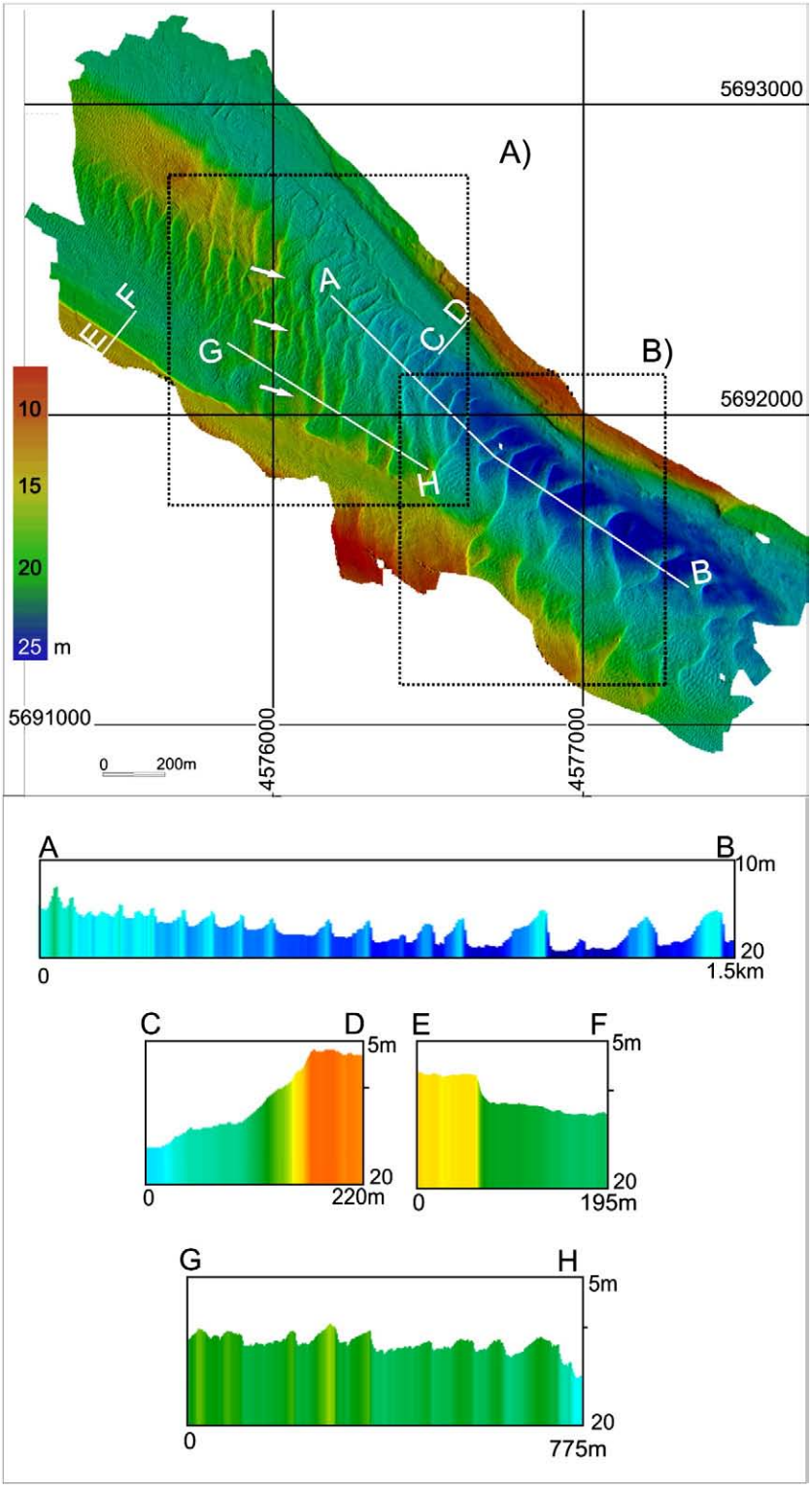


**Fig. 3.** Morphological map showing different topographic profiles and their location. White arrows point to the N–S orientation of the dune crest lines. The dotted line boxes represent Zones A and B as are shown in Fig. 6.

In tide-dominated estuaries, the superposition of smaller dunes on both stoss and lee sides of the larger ones is common. The entire study area, as well as the bank located northward, is covered with small 2D and 3D bedforms about 0.20 m in height, and as large as 1 m, with crest separations between 8 and 11 m. The crest line of these small bedforms exhibits a noticeable angle to the larger ones. They equilibrate relatively quickly with the flow as was mentioned previously by Dalrymple and Rhodes (1995), so they reverse with the semi-diurnal tidal period. All Large Dunes and Very Large Dunes are ebb-oriented, indicating residual sediment transport of the estuary (Fig. 3).

Two distinctive dune morphologies are evidenced by plotting $L$ vs $H$ (Fig. 4A). Very Large Dunes ($H>4$ m and $L>100$ m) are separated from others of smaller magnitude. The first ones are present only in Zone B and both dune types appear to happen under differing environmental

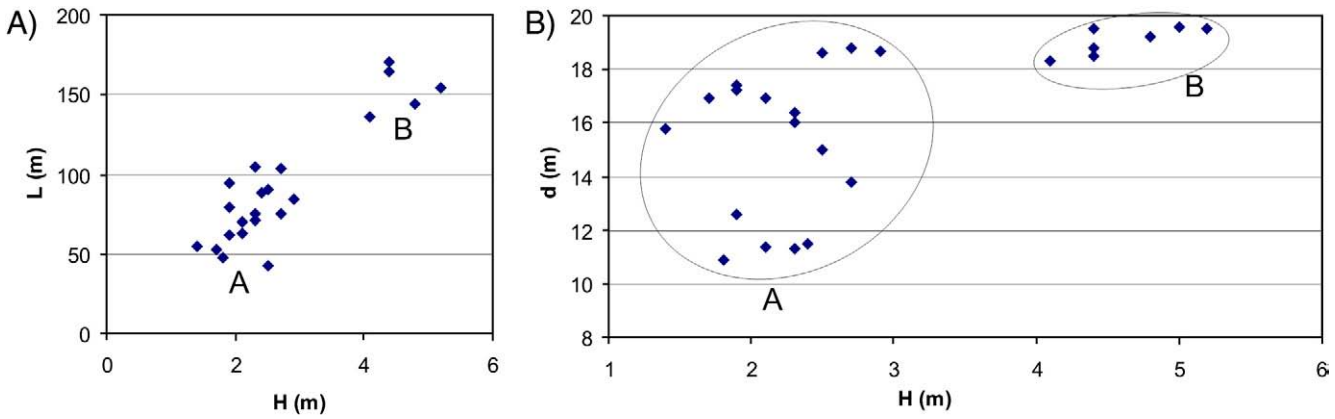


**Fig. 4.** Plot of dune morphology referred to Zones A and B (see Fig. 2 for location). A) Height ($H$) vs wavelength ($L$). B) Height ($H$) vs depth ($d$).

conditions. Plotting the dune height versus depth (Fig. 4B), it can be seen that Very Large Dunes only take place in depths between 18 m and 20 m (characteristically of Zone B), while Large Dunes, with height smaller than 3 m, occur in depths between 10 m and 19 m (typically of Zone A).

On the other hand, the fraction of the bed covered by moveable sediment (fullbeddedness) mentioned as descriptor of third order in the classification of Ashley (1990) can influence the dune formation. The underlying hard substrate prevents the erosion in the dune troughs giving them a flat base that can be considered as an effect of sediment starvation (Dalrymple and Rhodes, 1995). In the studied area, the maximum depth is geologically controlled by consolidated or lithified material, probably the Chasicó Fm. that also crops out south of this area (Perillo et al., 2009). Therefore, the thickness of the upper layer of sand is limited. At the northern boundary of the dune field, where maximum depths occur (Fig. 3) Very Large Dunes are formed, having a flat base (Fig. 3, profiles A–B) confirming the above-mentioned effect of sediment starvation.

### 4.2. Hydrodynamics

Tidal currents were measured by means of an ADCP during a whole cycle over two profiles located in Zones A and B, respectively (Fig. 5). In general, ebb currents are greater than flood ones; however, there are differences between Zone A and Zone B. In Zone B, maximum current speeds are greater than those occurring at Zone A. Fig. 5B shows that the areas on the northern flank (right side of the graph) characterized by current velocities greater than 125 cm $s^{-1}$ are greater than those measured in Zone A (Fig. 5A). This might be due to the narrowing of the channel in Zone B where the flanks are composed of hard Pliocene sediments that are difficult to erode. This fact indeed influences tidal currents by increasing the ebb speed in order to maintain the flow, which in turn, causes the deepening of the channel. The current increase in velocity together with sediment availability might be responsible of the formation of Very Large Dunes in Zone B.

On the other hand, there are noticeable differences within each zone. In Zone A (Fig. 5A) maximum values during both tidal stages are clustered in two well-defined loci along the section. This behaviour is probably related to the local topography, a submarine bank of 8-m depth (see Fig. 2). During the flood stage, the upstream widening of the channel may induce the sandbank build-up, which at the time makes the flow diverge, whereas during ebb the presence of such a sandbank may be conditioning the flow to remain separated downstream. Contrarily, in Zone B (Fig. 5B) maximum current speeds occur on the northern flank, where maximum depths are located and underlying rock crops out over a limited area.

### 4.3. Bedload transport

Sediment transport calculations instead of just tidal current speed were employed to analyse the factors leading to the particular dune morphologies. For this purpose, two facts were taken into account; namely, that the generation of bedrock is related only to those current velocities higher than the critical sediment shear stress, and that sediment transport as bed load increases with the cube of excess in current speed.

To quantify differences in sediment transport as bed load in the zone, the current velocities obtained over the two channel cross-sections were used. Even though these measurements correspond just to one tidal cycle, they are likely to represent the most important and frequently occurring conditions in the area as the measurements were made during spring tides.

The bedload transport model employed here was the algorithm proposed by Bagnold (1963) and modified by Gadd et al. (1978):

$$Q = \beta(U_{100} - U_{100c})^3$$

where $U_{100}$ is the velocity of the current and $U_{100c}$ is the critical velocity, both at 1 m above the bottom, and where $\beta$ is a parameter which depends on the grain size. It is well known that this algorithm gave the best agreement with observed sediment transport rates (Heathershaw, 1981). However, by comparing measured and computed transport rates, the accuracy of that predictor was notably increased by Gómez et al. (2006) who computed the substantially improved relationship for $\beta$ given below:

$$\beta = -4.057 D_{50} + 3.547$$

where $D_{50}$ is the median grain size, in our case with a value of 0.28 mm.

The deepest current measurements were acquired by the ADCP about 1.5 m above the seabed. Thus, the velocities at 1 m ($U100$) needed to compute bedload transport were calculated using the law of wall:

$$U_{100} = u_z \ln(1/z_0) / \ln(z/z_0)$$

where $z_0$ is the bottom roughness length (Nikuradse, 1933):

$$z_0 = kb/30$$

kb is the bed roughness height, which was defined as kb = $D_{50}$ + 3 Rh by Jonsson (1966). Rh is the bedform roughness height that can be measured from the observed bedform morphology obtained by the PMBS survey.

$U_{100c}$ was computed considering the critical shear stress ($\tau_{*c}$) which was calculated using Yalin (1977), which have been shown to

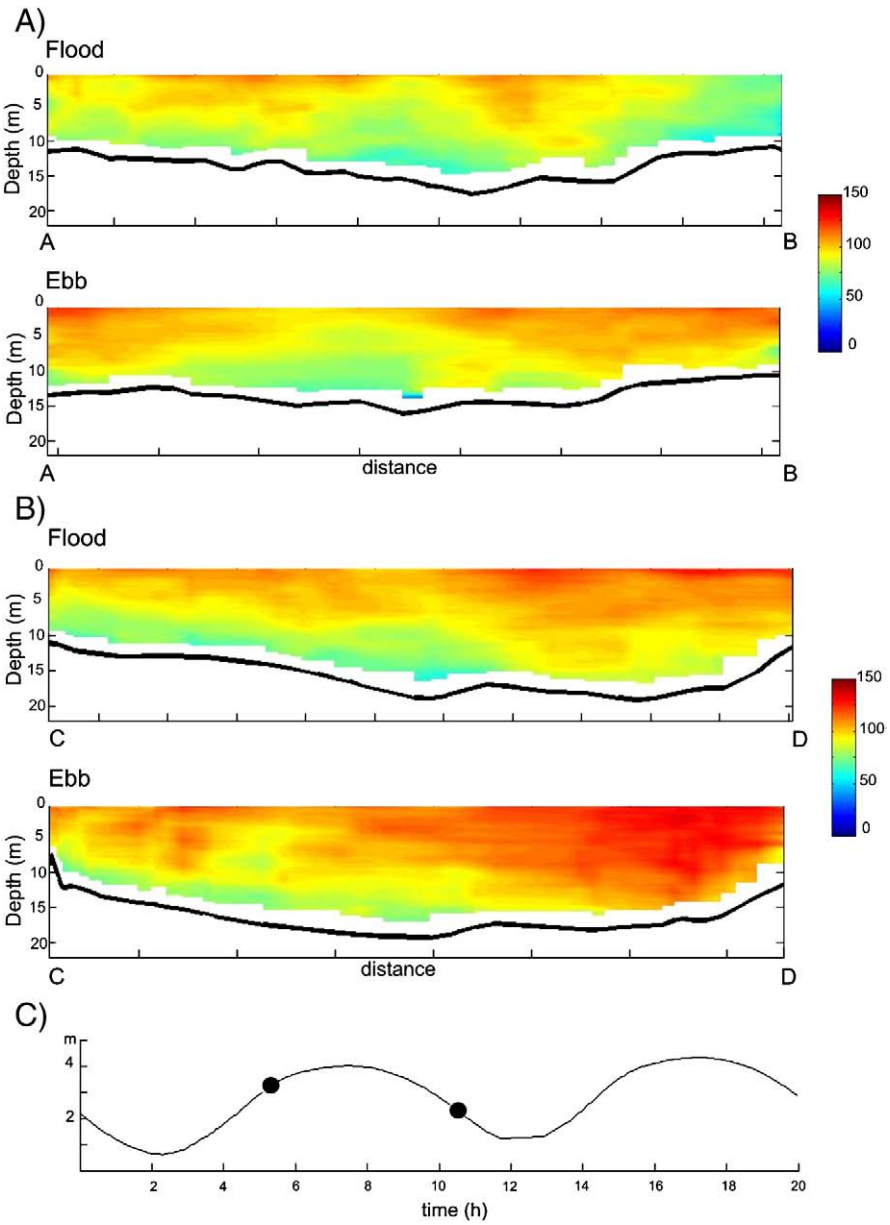


**Fig. 5.** Maximum tidal current velocity in cross-channel profiles obtained by means of ADCP (see Fig. 6 for profile location) during flood and ebb tidal conditions. A) Profile in Zone A. B) Profile in Zone B. C) Tidal height during the survey. The circles indicate the flood and ebb conditions where the profiles were measured. Current velocity is in cm $s^{-1}$. Extremes A and C are located on the southern channel flank and B and D are on its northern flank.

be in reasonable agreement with laboratory results concerning bioclastic sands (Paphitis et al., 2002):

$$\tau_{*_c} = \theta_t(\rho_s - \rho)gD_{50}$$

where $\theta_t$ is the Shields parameter, $\rho_s$ and $\rho$ are sediment and water density, respectively, and g is acceleration due to gravity.

Then, $U_{100c}$ was calculated (Li and Amos, 1995) as:

$$U_{100c} = \left(\tau_{*c}/0.5\rho\right)^{0.5}$$

where fc = 0.006 is the current friction factor, following Sternberg (1972).

Examples of the computed sand transport as bedload are shown in Fig. 6. These results were obtained from the maximum values for both tidal stages, ebb and flood, measured during spring tides. In Fig. 6, it is possible to appreciate that on both tidal stages, maximum sand transport rates in Zone B is noticeably greater than in Zone A. In addition, in both zones, sand transport is greater during the ebb than during the flood. However, the analysis of sand transport rates during both tidal stages, led us to appreciate some particular characteristics. In Zone B, maximum sand transport rates take place where maximum depths occur, with values of the order of 2 kg $m^{-1}$ $s^{-1}$ during ebb. These maximum values occur on the northern flank, where the availability of sand is sufficient to form Very Large Dunes. The narrowing of the area caused by a geological control, where the channel exhibits its greater depths, produces an increase in the tidal currents, which immediately translates into higher bedforms. This particular geological control appears to be the explanation for the formation of that type of dunes in this mesotidal estuary.

On the other hand, Dalrymple and Rhodes (1995) suggested that confinement of the tidal currents by channel banks produces rectilinear flow; thus, most tidal dunes should be nearly transverse to both, the ebb and flood currents, and to the direction of residual transport. For that reason, it is widely assumed that dune crest lines are perpendicular to the strongest (dominant) current or residual

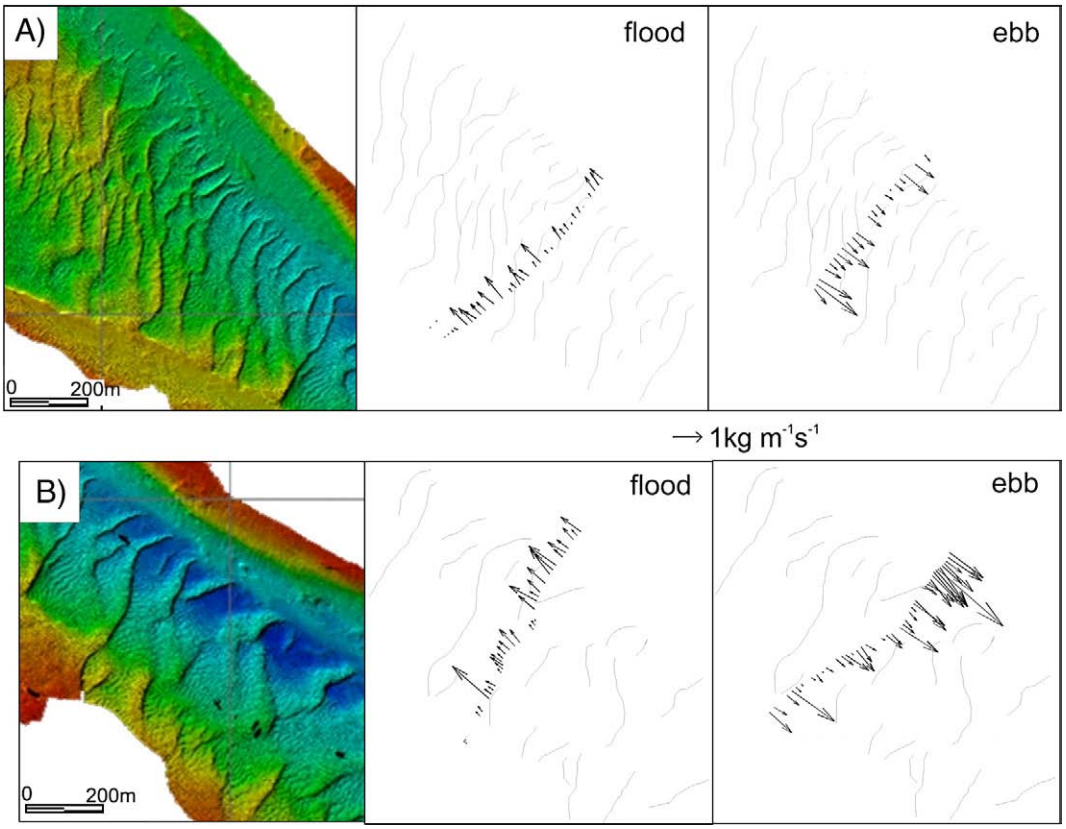


**Fig. 6.** Arrows show maximum sediment transport as bedload obtained for the cross-channel profiles of tidal current speeds. A) Zone A. B) Zone B (see Fig. 3 for zone location). Drawn lines show the crests of the dunes where values of bedload transport for flood and ebb tidal conditions are superimposed.

sediment transport direction. However, the submarine morphology of the Zone A shows Large and Medium Dune crest lines oblique to the current direction (Fig. 6) and subsequently to the channel axis. Such obliquity might be explained by the differential sand transport occurring in the area. Maximum transport rates during ebb exceed maximum flood transport rates in the entire section. However, the transport rate during the ebb is notably greater on the southern flank than in the northern flank. This difference would lead to dune crest-line obliquity first and eventually lead to separation into differing dunes downstream.

### 4.4. Dune migration rates

In Zone B, where larger bedforms occur, it was possible to measure the dune migration rate. It was done by comparing the bathymetry of the area carried out eight months apart by means of the GeoSwath Plus specific software (GS+ v3.10), which allows us to measure and compare bathymetric maps with high accuracy (centimetres in height and position). Thus, the larger dunes of the area were clearly and easily identified in both bathymetric maps, as they show almost the same general shape in both surveys, but downstream displaced, as can be seen in Fig. 7. The displacement of each particular dune was computed by measuring the distance between the dune's crest line middle points in both grids. Taking into account the eight months that lapsed between the elaborations of the two maps, the migration rate (distance per year) was calculated for ease of comparing with previous studies. The entire dune field shows a direct downstream migration due to predominance of ebb-oriented sediment transport.

The measured migration rate ranged from 65 m year$^{-1}$ to 135 m year$^{-1}$ and depends mainly on the dune height. In general, the Very Large Dunes located on the northern flank migrated at a slower velocity than the Large Dunes present on the southern flank. The migration rate for Large Dunes ranged from 80 to 130 m year$^{-1}$, whereas for Very Large Dunes it was between 65 and 96 m year$^{-1}$. The difference probably is due to the major volume of sediment the Very Large Dunes needs to move and considering that the transport rate is the same over all bedforms, the larger ones will move more slowly. All these values are notably larger than the 32 m year$^{-1}$ given by Aliotta and Perillo (1987) for a nearby dune field within the estuary. These authors computed such a value by means of two successive side-scan sonar surveys performed six months apart that were positioned by a microwave-based method (Trisponder), with a high total combined error. Moreover, the values measured in the present study are greater than the compilation reported by Dalrymple and Rhodes (1995) for the same type of dunes around the world. In general, these authors assumed that dunes between 0.5 and 5 m high commonly migrate 25–75 m year$^{-1}$, while dunes with heights greater than 3 m may have rates of only a few decimeters per year. Among those studies, for dune sizes similar as the ones found here from different estuaries (dunes in rivers are excluded), we note migration rates as low as 25 m year$^{-1}$ in the Thames estuary for dunes of 1.5–8 m height (Langhorne, 1973) and 0.35 m year$^{-1}$ for dunes of 4–16.5 m height found in the flood tidal delta of Long Island Sound (Fenster et al., 1990).

## 5. Summary and conclusions

There are two different and well-defined zones characterized by particular dune morphology. Both areas have differing hydrodynamic profiles, important lateral and vertical variations in tidal current velocities and direction. In the upstream zone characterized by Medium and Large Dunes, the crest lines exhibit an angle with the main current direction. The responsible mechanism would be the differential transport rate across the channel, which at the time leads to a non-uniform migration rate along the dune crest line. The channel narrowing

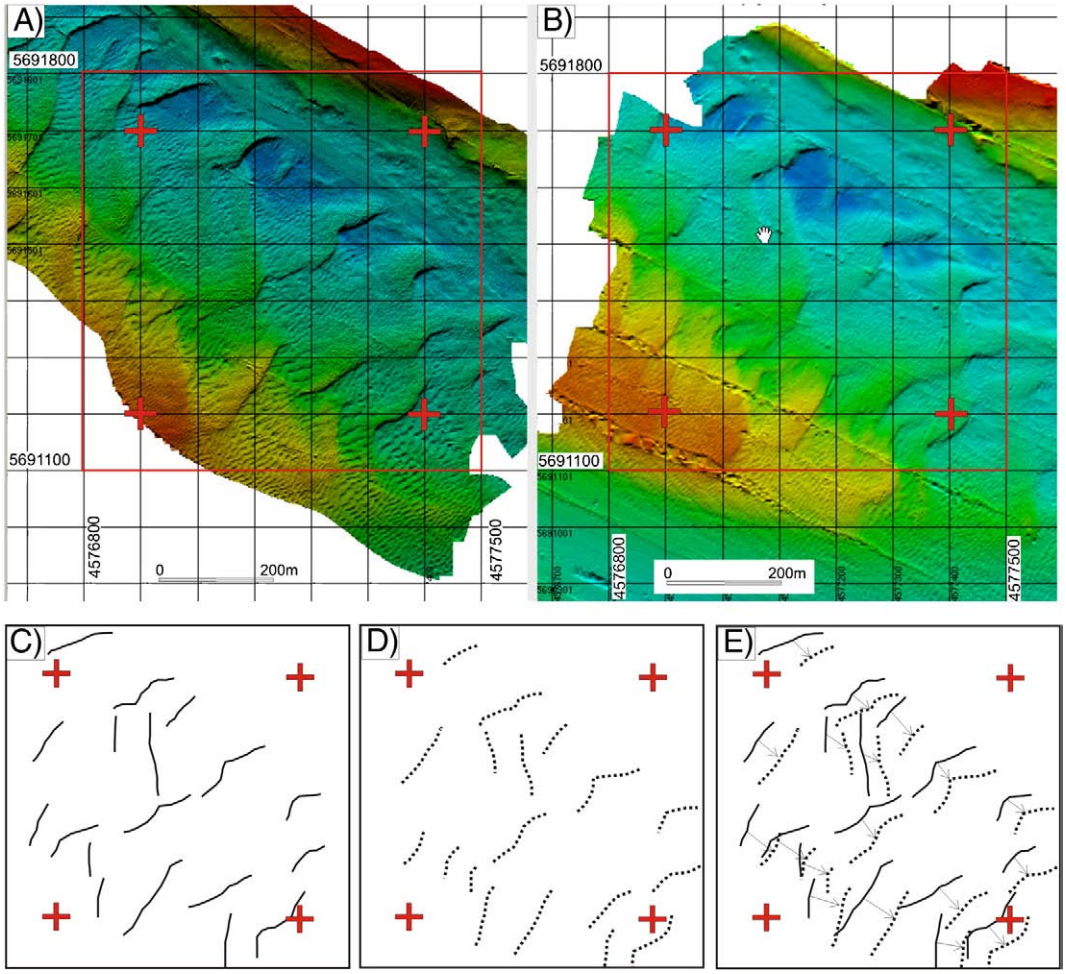


**Fig. 7.** Bathymetric maps comparison on Zone B (see Fig. 3). A) September, 2007. B) May, 2008. C) Drawn solid lines represent dune crest lines in September, 2007. D) Drawn dotted lines represent dune crest lines in May, 2008. E) Comparison between both periods showing dune displacement by means of the arrows. The cross marks indicate the same position for comparative purposes.

owing to the presence of sediment that is hard to erode at 10-m depth, produces a non-uniformity in the net sediment transport along the channel cross-section. Nevertheless, the presence of a linear crest oblique to the tidal currents direction indicates that determining the direction of net sediment transport just through the orientation of large bedforms may be subject to a significant error. More studies and measurements are necessary to confirm the proposed mechanism.

The geological control affects the dynamics of the entire area, even the bedforms characteristics. The reduction in the channel cross-section leads to an increase in tidal current speeds. This acceleration deepens the channel up to the underlying highly compacted and cemented Pliocene sediments and form Very Large Dunes characterized by an asymmetrical profile oriented towards the estuary mouth. An increase in current velocity leads to an increase in dune height and wavelength, with a flat base in between. This morphology is typical when limited amounts of sediment overlie a rigid substrate.

The migration rates of the bedforms measured in this study decreases as the bedform height increases, being typically in the order of 80–130 m year$^{-1}$ for Large Dunes and 65–96 m year$^{-1}$ for Very Large Dunes. These values are greater than those previously measured in the area and are even larger than those maximum values from other similar environments worldwide.

Finally, we note that the unusual presence of Very Large Dunes in a mesotidal estuary, as well as the large migration rates measured here, are the particular consequence of tidal current speed enhancement promoted by the narrowing of the channel as a consequence of a local geological control.

## Acknowledgements

The authors gratefully thank Ernesto Alberdi for the current data acquisition. Also, thanks to the vessel crew Camilo Bernardez, Enio Redondo and Alberto Conte for their assistance in fieldwork. This paper was significantly improved by the comments of J. Ollerhead and an anonymous journal referee. This research was supported by PICT 00109 and PICT 1878 of the Agencia Nacional de Promocion Cientifica y Tecnológica and PGI 24/ZH15 from the Secretaría Ciencia y Tecnologia-UNS.

## References

Aliotta, S., Perillo, G.M.E., 1987. A sand wave field in the entrance to the Bahía Blanca estuary, Argentina. Mar. Geol. 76, 1–14.
Allen, J.R.L., 1982. Sediment structures: their character and physical basis. Developement in Sedimentology Series, vol. 30. Elsevier, New York, p. 593.
Ardhuin, F., Drake, T.G., Herbers, T.H.C., 2002. Observations of wave-generated vortex ripples on the North Carolina continental shelf. J. Geophys. Res. 107 (C10), 3143. doi:10.1029/2001JC000986.
Ashley, G.M., 1990. Classification of large scale subaqueous bedforms: a new look at an old problem. J. Sediment. Petrol. 60, 160–172.
Bagnold, R.A., 1963. Mechanics of marine sedimentation. In: Hill, M.N. (Ed.), The Sea, Vol. 3. Wiley-Interscience, New York, pp. 507–582.
Bartholdy, J., Flemming, B.W., Bartholoma, A., Ernstsen, V.B., 2005. Flow and grain size control of depth-independent simple subaqueous dunes. J. Geophys. Res. 110, F04S16. doi:10.1029/2004/JF000183.
Bastos, A.C., Paphitis, D., Collins, M.B., 2004. Short-term dynamics and maintenance processes of headland-associated sandbanks: Shambles Bank. English Channel, UK. Estuar. Coast. Shelf Sci. 59, 33–47.

Besio, G., Blondeaux, P., Brocchini, M., Vittori, G., 2004. On the modeling of sand wave migration. J. Geophys. Res. 109, C04018. doi:10.1029/2002JC001622.
Blott, S.J., Pye, K., 2001. GRADISTAT: a grain size distribution and statistics package for the analysis of unconsolidated sediments. Earth Surf. Processes Landforms 25, 1237–1248.
Carling, P.A., Golz, E., Orr, H.G., Radecki-Pawlik, A., 2000. The morphodynamics of fluvial sand dunes in the River Rhine, near Mainz, Germany. Part I. Sedimentology and morphology. Sedimentology 47, 227–252.
Cuadrado, D.G., Gómez, E.A., Ginsberg, S.S., 2003. Large transverse bedforms in a mesotidal estuary. Rev. Argent. Sedimentol. 10, 163–172.
Cuadrado, D.G., Gómez, E.A., Ginsberg, S.S., 2005. Tidal and longshore sediment transport associated to a coastal structure. Estuar. Coast. Shelf Sci. 62, 291–300.
Dalrymple, R.W., Knight, R.J., Lambiase, J.J., 1978. Bedforms and their hydraulic stability relationships in a tidal environment, Bay of Fundy, Canada. Nature 275, 100–104.
Dalrymple, R.W., Rhodes, R.N., 1995. Estuarine dunes and bars. In: Perillo, G.M.E. (Ed.), Geomorphology and Sedimentology of Estuaries: Developments in Sedimentology, 53. Elsevier, Amsterdam, pp. 359–422.
Ernstsen, V.B., Noormets, R., Winter, C., Hebbeln, D., 2005. Development of subaqueous barchanoid-shaped dunes due to lateral grain size variability in a tidal inlet channel of the Danish Wadden Sea. J. Geophys. Res. 110, F04S08. doi:10.1029/2004JF000180.
Fenster, M.S., Fitzgerald, D.M., Bohlen, W.F., Lewis, R.S., Baldwing, C.T., 1990. Stability of giant sand waves in eastern Long Island Sound, U.S.A. Mar. Geol. 91, 207–225.
Flemming, B.W., 1978. Underwater sand dunes along the southeast African continental margin—observations and implications. Mar. Geol. 26, 177–198.
Francken, F., Wartel, S., Parker, R., Taverniers, E., 2004. Factors influencing subaqueous dunes in the Scheldt Estuary. Geo-Mar. Lett. 24, 14–24.
Gadd, P.E., Lavelle, J.W., Swift, D.J.P., 1978. Estimates of sand transport on the New York shelf using near-bottom current meter observations. J. Sediment. Petrol. 48, 239–252.
Goff, J.A., Kraft, B.J., Mayer, L.A., Schock, S.G., Sommerfield, C.K., Olson, H.C., Gulick, S.P.S., Nordfjord, S., 2004. Seabed characterization on the New Jersey middle and outer shelf: correlatability and spatial variability of seafloor sediment properties. Mar. Geol. 209, 147–172.
Gómez, E.A., Amos, C.L., Li, M.Z., 2006. Evaluation of sand transport models by in situ observations under unidirectional flow. J. Coastal Res. SI 39, 578–581.
Harbor, D.J., 1998. Dynamics of bedforms in the lower Mississippi River. J. Sediment. Res. 68, 750–762.
Heathershaw, A.D., 1981. Comparisons of measured and predicted sediment transport rates in tidal currents. Mar. Geol. 42, 75–104.
Jonsson, I.G., 1966. Wave boundary layers and friction factors. Proceedings 10th International Coastal Engineering Conference (Tokyo, Japan), I, pp. 127–148.
Kostaschuk, R.A., Church, M.A., Luternauer, J.L., 1989. Bedforms, bed material, and bedload transport in a salt-wedge estuary: Fraser River, British Columbia. Can. J. Earth Sci. 26, 1440–1452.
Langhorne, D.N., 1973. A sandwave field in the outer Thames estuary, Great Britain. Mar. Geol. 14, 129–143.
Li, M.Z., Amos, C.L., 1995. SEDTRANS92: a sediment transport model for continental shelves. Comput. Geosci. 21, 533–554.
Mitchell, N.C., 1996. Processing and analysis of Simrad multibeam sonar data. Mar. Geophys. Res. 18, 729–739.
Nikuradse I., 1933. Strömungsgesetze in rauhen Röhten. *VDI-Forschungscheft* No. 361.
Paphitis, D., Collins, M.B., Nash, L.A., Wallbridge, S., 2002. Settling velocities and entrainment thresholds of biogenic sands (shell fragments) under unidirectional flow. Sedimentology 49, 211–225.
Perillo, G.M.E., Piccolo, M.C., 1991. Tidal response in the Bahía Blanca Estuary. J. Coast. Res. 7, 437–449.
Perillo, G.M.E., Gómez, E.A., Cuadrado, D.G., Alberdi, E., Vitale, A., Piccolo, M.C., 2009. Geomorphology and sediment dynamics of the middle reach of the Bahía Blanca. In: Vionnet, C.A., García, M.H., Latrubesse, E.M., Perillo, G.M.E. (Eds.), River, Coastal and Estuarine Morphodynamics. Balkema, London, pp. 237–241.
Rubin, D.M., McCulloch, D.S., 1980. Single and superimposed bedforms: a synthesis of San Francisco Bay and flume observations. Sediment. Geol. 26, 207–231.
Sternberg, R.W., 1972. Predicting initial motion and bedload transport of sediment particles in the shallow marine environment. In: Swift, D.J.P., Duane, D.B., Pilkey, O.H. (Eds.), Shelf Sediment Transport: Process and Pattern, Dowden. Hutchinson & Ross, Stroudsburg, pp. 61–82.
Sukhodolov, A., Thiele, M., Bungartz, H., 1998. Turbulence structure in a river reach with sand bed. Water Resour. Res. 34, 1317–1334.
Xu, J.P., Wong, F.L., Kvitek, R., Smith, D.P., Paull, C.K., 2008. Sandwave migration in Monterey Submarine Canyon, Central California. Mar. Geol. 248, 193–212.
Yalin, M.S., 1977. Mechanics of Sediment Transport. Pergamon Press, Oxford. 298 pp.